Title: Digital holography for quantitative phase-contrast imaging

Etienne Cuche, Frederic Bevilacqua, and Christian Depeursinge
Institute of Applied Optics, Swiss Federal Institute of Technology, CH-1015 Lausanne, Switzerland

Presenter: Nitin Rawat

The holographic process is described mathematically as follows:

$$O(x,y) = o(x,y)\,\mathrm{e}^{i\varphi_o(x,y)} \quad \text{... (1.1)}$$

Is the complex amplitude of the object wave with real amplitude o and phase φ_o and

$$R(x,y) = r(x,y)\,\mathrm{e}^{i\varphi_R(x,y)} \quad \text{... (1.2)}$$

Is the complex amplitude of the reference wave with real amplitude r and phase φ_R

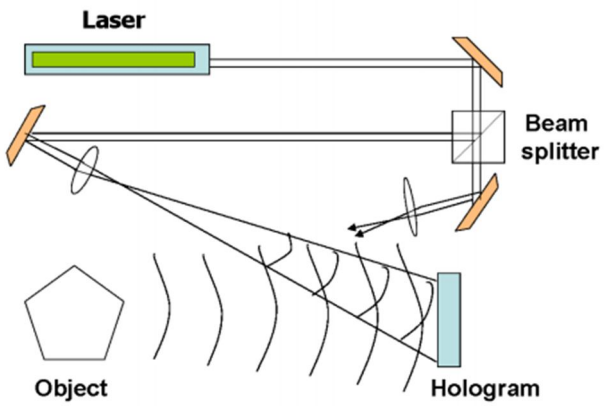

Fig. 1 Construction of a hologram

Both waves interfere at the surface of the recording medium. The intensity is calculated by

$$\begin{aligned} I_H(x,y) &= \left|O(x,y)+R(x,y)\right|^2 \\ &= (O(x,y)+R(x,y))(O(x,y)+R(x,y))^* \\ &= R(x,y)R^*(x,y)+O(x,y)O^*(x,y) \\ &+ O(x,y)R^*(x,y)+R(x,y)O^*(x,y) \end{aligned} \quad \text{... (1.3)}$$

Digital Recording

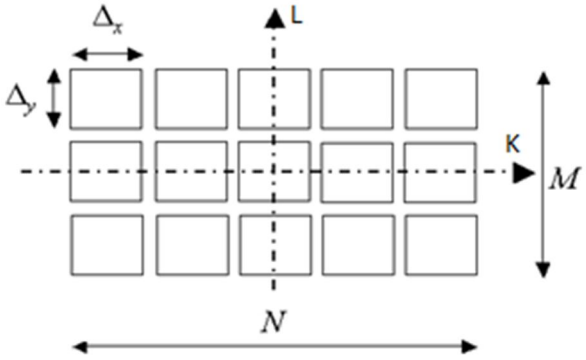

Fig. 2 Concept diagram of a surface-pixel sensor

The digital recording will (depending on the directions x and y on the recording plane) consist of M x N pixels. Each of these pixels is of a dimension $\Delta_x \times \Delta_y$. In CCD sensors, Matrices made up of photosensitive elements called pixels are generally square-shaped. In our case it is $12 \times 12 \mu m$

In their case, the hologram intensity was recorded by a standard black and white CCD camera (Hitachi Denshi KP-M2).

The two neutral-density filters allow the adjustment of the object and the reference intensities.

A square image of area LxL (Sensor size) = 4.83mm X 4.83mm containing N x N= 512 x 512 pixels is acquired in the center of the CCD sensor, and a digital hologram is transmitted to a computer via a frame grabber.

The digital hologram $I_H(k,l)$ results from two-dimensional spatial sampling of $I_H(x,y)$ by the CCD:

$$I_H(k,l) = I_H(x,y) rect\left(\frac{x}{L}, \frac{y}{L}\right) \times \sum_{k}^{N} \sum_{l}^{N} \delta(x - k\Delta x, y - l\Delta y) \quad \text{... (1.5)}$$

Where k and l are integers $(-N/2 \le k,l \le N/2)$ and Δx and Δy are the sampling intervals in the hologram plane i.e. pixel size: $\Delta x = \Delta y$ =L/N

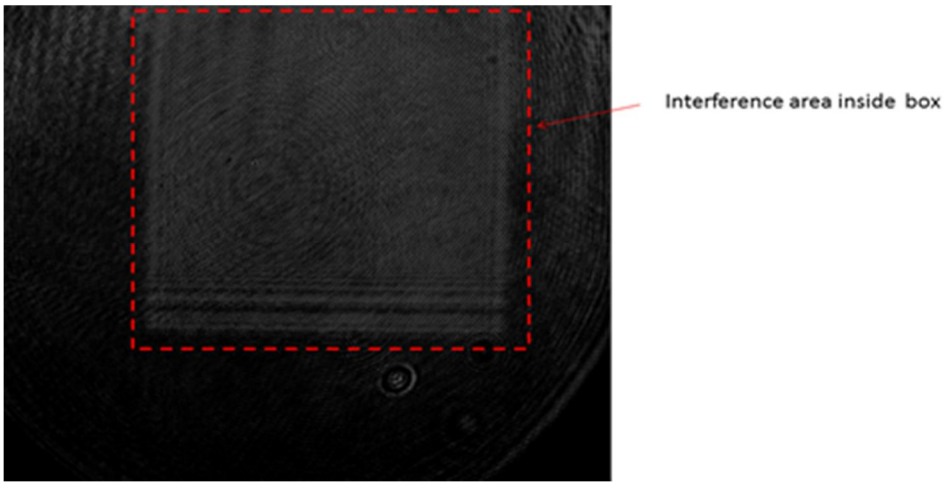

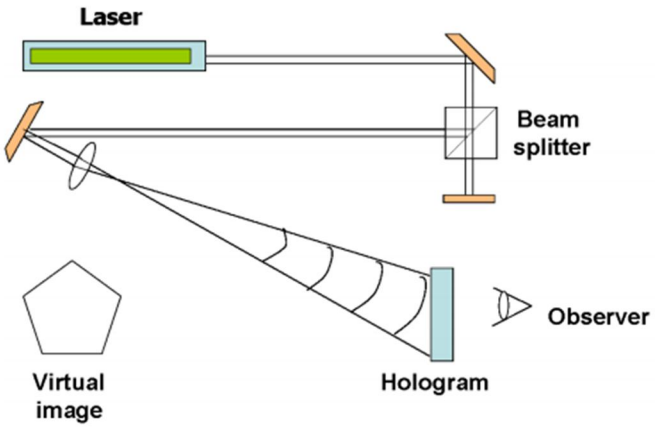

Fig.3 Reconstruction of a hologram

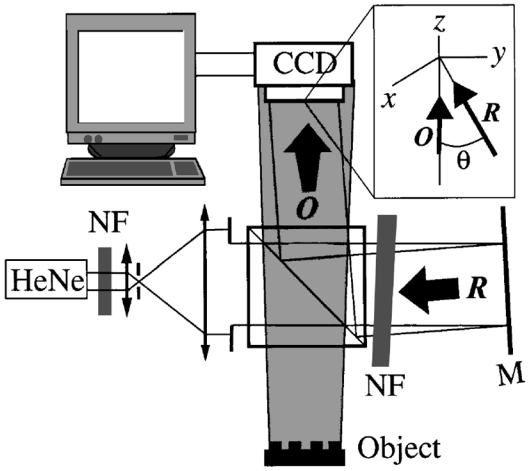

Fig.4 Experimental setup

A wave front $\psi_H(x,y) = R(x,y)I(x,y)$ is transmitted by a hologram and propagates toward an observation plane, where a three-dimensional image of the object can be observed.

For reconstructing a digital hologram, a digital transmitted wave front $\psi_H(k\Delta x, l\Delta y)$ is computed by multiplication of digital hologram $I_H(k,l)$ by a digital computed reference wave, $R_D(k,l)$,called the digital reference wave.

Taking into account the definition of hologram intensity [Eq. 1.3], we have

$$\psi\ (k\Delta x, \Delta y) = R_D(k,l)I_H(k,l) \qquad \text{... (1.7)}$$

$$= \underbrace{R_D\left|R\right|^2 + R_D\left|O\right|^2}_{Zero\ order\ of\ diffraction} + \underbrace{R_D R^* O}_{Twin\ image} + \underbrace{R_D R O^*}_{real\ image}$$

To avoid an overlap of these three components of ψ during reconstruction, they recorded the hologram in the so-called off-axis geometry. For this purpose the mirror in the reference arm, M is oriented such that the reference wave **R** reaches the CCD at an incidence angle θ .The value θ must be sufficiently large to ensure separation between the real and the twin images in the observation planes. However, θ must not exceed a given value so that the spatial frequency of the interferogram does not exceed the resolving power of the CCD.

$$\theta \le \theta_{\max} = arc\ \sin\left(\frac{\lambda}{2\Delta x}\right) \qquad \text{... (1.8)}$$

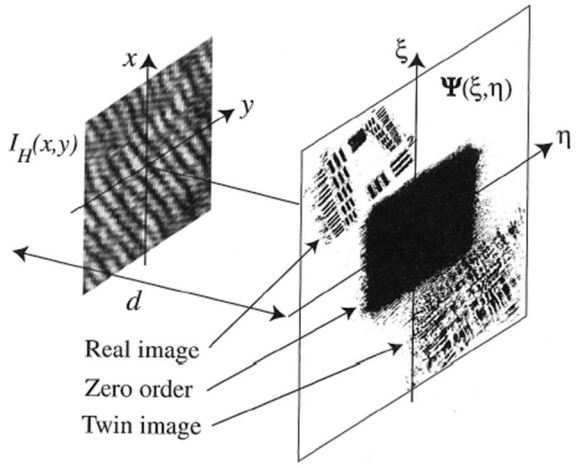

Geometry for hologram reconstruction. *0xy*, hologram plane; *0*ξη, observation plane; *d*, reconstruction distance; **Ψ**(ξ, η), reconstructed wave front.

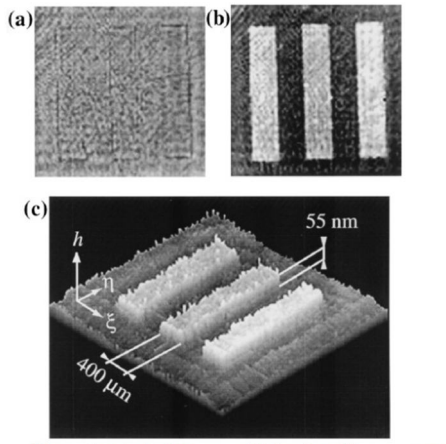

Reconstructed images obtained with a pure phase object: (a) amplitude contrast, (b) phase contrast, (c) three-dimensional perspective of the reconstructed height distribution (the vertical scale is not equal to the transverse scale).

The reconstructed wave front $\psi(m\Delta\xi, n\Delta\eta)$, at a distance d from the hologram plane, is computed by use of a discrete expression of the Fresnel integral:

$$\psi(m\Delta\xi, n\Delta\eta) = A\exp\left[\frac{i\pi}{\lambda d}(m^2\Delta\xi^2 + n^2\Delta\eta^2)\right] \times FFT\left\{R_D(k,l)I_H(k,l)\exp\left[\frac{i\pi}{\lambda d}(k^2\Delta x^2 + l^2\Delta y^2\right]\right\}_{m,n} \quad \text{... (1.9)}$$

Where m and n are integers $(-N/2 \le m, n \le N/2)$, FFT is the fast Fourier transform operator, and $A = \exp(i2\pi d/\lambda)/(i\lambda d)$

$\Delta\xi$ and $\Delta\eta$ are the sampling intervals in the observation plane and define the transverse resolution of the reconstructed image.

This transverse resolution is related to the size of the CCD (L) and to the distance d by,

$$\Delta\xi = \Delta\eta = \lambda d / L \quad \text{... (1.10)}$$

The reconstructed wave front is an array of complex numbers. The amplitude and the phase contrast images can be obtained by calculation of the square modulus.

A new (semantic) reflexive brain–computer interface: In search for a suitable classifier

A. Furdea et al. University of Tubingen, Germany

Journal of Neuroscience Methods (2012)

Presenter : Younghak Shin
GIST, Dept. of Information and Communication, INFONET Lab.

Gwangju Institute of Science and Technology

Objective

- The goal of this study is to find a suitable classifier for EEG data derived from a new learning paradigm which aims at communication in paralysis.
- A reflexive semantic classical (Pavlovian) conditioning paradigm is explored as an alternative to the operant learning paradigms, currently used in most BCIs.
- Four classification algorithms are compared for classifying off-line data collected from a group of 14 healthy participants
  - stepwise linear discriminant analysis (SWLDA)
  - shrinkage linear discriminant analysis (SLDA)
  - linear support vector machine (LIN-SVM)
  - radial basis function kernel support vector machine (RBF-SVM)

Introduction

- BCIs provide a non-muscular communication channel for individuals who are no longer able to communicate due to severe physical impairment.
- Over the last years it has been shown that patients with severe motor disability are able to control an EEG based BCI (e.g. sensori-motor rhythm (SMR) and P300)
- However, there are no documented cases of CLIS(completely locked-in state : all motor control is lost) patients communicating by means of BCI
- It has been suggested that a paradigm shift from instrumental-operant learning to classical conditioning is necessary to overcome the failure of CLIS patients to achieve BCI control
- The aim of this study is to find a suitable classifier and to assess the relative performance of four classification techniques on EEG data derived from a classical conditioning paradigm.

Introduction

- Classical conditioning (Pavlovian conditioning)

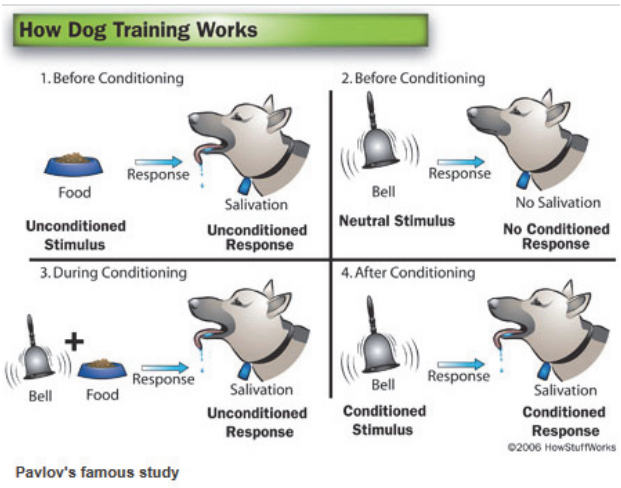

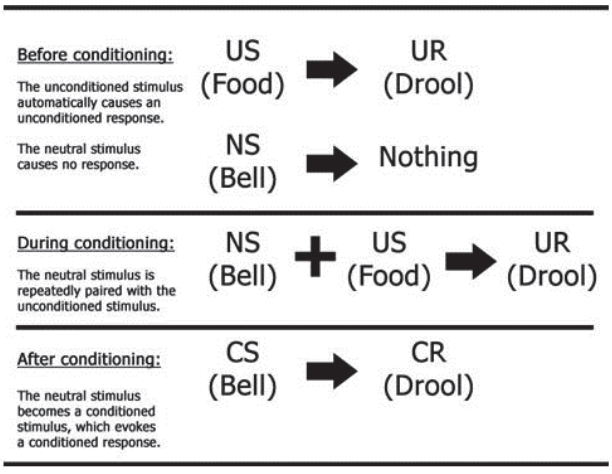

http://drlack.wikispaces.com/Principles+of+Learning

Data collection

- Participants
  - Fourteen healthy participants (8 women and 6 men, mean age 24.36, SD 5.4, range 21–42) took part in this study
- Task procedure and design
  - All participants took part in two experimental sessions
  - Each session was divided into three blocks, each block consisted of 50 true and 50 false sentences, i.e. trials.
  - In each block, the sentences were presented in random order through earphones.
  - The conditioned stimuli (CS) were either ‘yes’ or ‘no’ sentences, according to the type of the sentence (CS1 and CS2).

Data collection

- Task procedure and design

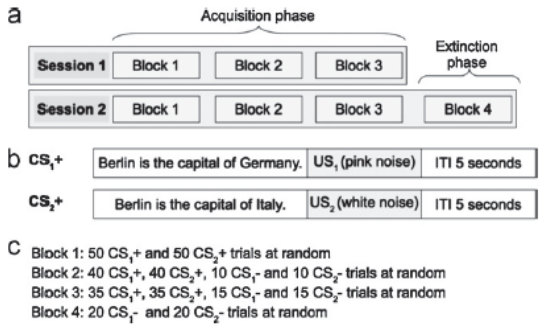

Fig. 2. The experimental design. (a) Session setup: blocks 1, 2 and 3 from sessions 1 and 2 are referred to as the *acquisition phase*; block 4 from session 2 is referred to as *extinction phase*. (b) An example of the conditioned stimuli CS_1+ and CS_2+. (c) Number of randomly presented trials per block.

  - To learn ‘yes-’ or ‘no-thinking’ two different unconditioned stimuli (US) were used:
    - a pink noise US1 immediately following a true sentence
    - a white noise US2 immediately following a negative sentence which produced the unconditioned brain response(UR)

Data collection

- Both US were set to have the same duration of 500 ms and were presented monaurally at different intensities.
- US1 was always presented to the right ear with an intensity of 75 dB and US2 was always presented to the left ear with an intensity of 105 dB.
- For each session, during the first block, every CS was paired with an US and denoted as CS1+ and CS2+.
- In the second block 10 CS, at random, were not paired with US1 and US2 and are referred to as CS1− and CS2−.
- In the third block 15 CS, at random, were not paired with US1 and US2.
- CS1- and CS2- are of a particular importance for on-line communication because in an on-line scenario only unpaired sentences can be used.
- At the end of the second session a fourth block of sentences was introduced, further referred to as the extinction phase.
- The purpose of this phase was to assess the lasting effects of conditioning.

Data acquisition and processing

Data collection

- stepwise Linear Discriminant Analysis

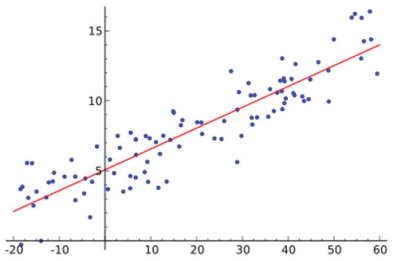

Example of simple linear regression

Methods

- Shrinkage LDA

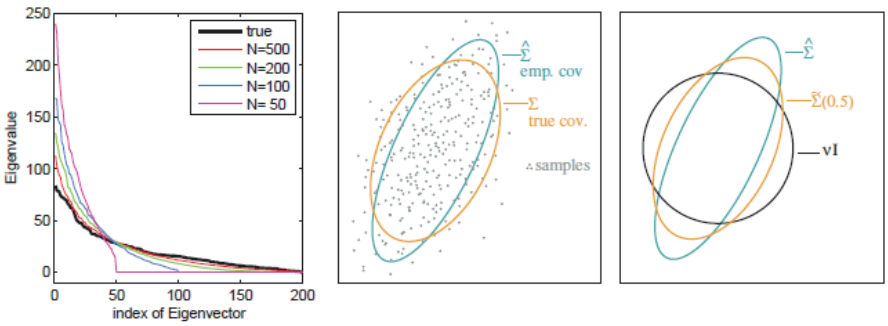

Figure 7: *Left:* Eigenvalue spectrum of a given covariance matrix (bold line) and eigenvalue spectra of covariance matrices estimated from a finite number of samples drawn (N= 50, 100, 200, 500) from a corresponding Gaussian distribution. *Middle:* Data points drawn from a Gaussian distribution (gray dots; d = 200 dimensions, two dimensions selected for visualization) with true covariance matrix indicated by an orange colored ellipsoid, and estimated covariance matrix in cyan. *Right:* An approximation of the true covariance matrix can be obtained as a linear interpolation between the empirical covariance matrix and a sphere of approriate size.

Thank you

Conditions for practicing compressive Fresnel holography

Speaker : Sangjun Park
Authors: Yair Rivenson* and Adrian Stern
{rivenson@ee.bgu.ac.il}

OPTICS LETTERS, 2011

INFONET Lab, Dept. of Information and Communication, GIST

Gwangju Institute of Science and Technology

Background- the coherence parameter μ

- The coherence parameter that measures the dissimilarity between the sensing matrix Φ and the sparsifying matrix Ψ is defined as

$$\mu(\Phi,\Psi) := \max_{k,j} \left| \langle \phi_k, \psi_j \rangle \right|.$$

- Then, CS theory asserts that the signal can be accurately reconstructed by taking m uniformly at random selected measurements, obeying

$$m \geq C\mu(\Phi,\Psi) s \log n$$

where C is a positive constant.

Backgrounds - the Fresnel approximation

- The Fresnel approximation is used for representing the complex values of a propagating wave measured in a planer perpendicular to the direction of propagation and separated by a distance **z**.

$$u_z(x) = u_{in} * \exp\left\{\frac{j\pi}{\lambda z}x^2\right\}$$

The one-dimensional Fresnel approximation

$$= \int u_{in}(\xi)\exp\left\{\frac{j\pi}{\lambda z}(x-\xi)^2\right\}d\xi$$

$$= \exp\left\{\frac{j\pi}{\lambda z}x^2\right\}\int u_{in}(\xi)\exp\left\{\frac{j\pi}{\lambda z}\xi^2\right\}\exp\left\{-\frac{2j\pi x\xi}{\lambda z}\right\}d\xi$$

The term is related to the Fourier transform

- Here, λ is the wavelength of the light wave and $u_{in}(\xi)$ is the input object.
- We refer the Fresnel approximation as the Fresnel transform.

Backgrounds - the form of the Fresnel transform depending on propagation distances.

- Let **z** be infinity.
- The Fresnel transform becomes the Fourier transform.

$$u(x) = \exp\left\{\frac{j\pi}{\lambda z}x^2\right\}\int u_{in}(\xi)\exp\left\{\frac{j\pi}{\lambda z}\xi^2\right\}\exp\left\{-\frac{2j\pi x\xi}{\lambda z}\right\}d\xi$$

$$\approx \exp\left\{\frac{j\pi}{\lambda z}x^2\right\}\int u_{in}(\xi)\exp\{0\}\exp\left\{-\frac{2j\pi x\xi}{\lambda z}\right\}d\xi$$

$$= \exp\left\{\frac{j\pi}{\lambda z}x^2\right\}\int u_{in}(\xi)\exp\left\{-2j\pi\xi\frac{x}{\lambda z}\right\}d\xi$$

$$= \exp\left\{\frac{j\pi}{\lambda z}x^2\right\}\mathcal{F}\left[u_{in}\left(\frac{x}{\lambda z}\right)\right]$$

- The complex values of the propagating wave are easily obtained by using the Fourier transform.

A problem statement

- Can we derive theoretical bounds on the performance of compressive imaging systems based on Fresnel wave propagation?

- The authors presented theoretical bounds in terms of imaging sensor's physical attributes, illumination wavelength, and working distance.

The definition of far-field and near-field regimes

- Let n be the number of object and CCD pixels.
- Let Δx_z be the object resolution element size, and Δx_z be the output field's pixel size.
- If the distance z obeys

$$z \geq n\Delta x_0^2 / \lambda$$

then we say that the distance z belongs to far-field regime.

- Otherwise, the distance z belongs to near-field regime.
- Also, there is the relation between the input and output pixel sizes should be

$$\Delta x_z = \lambda z / (n\Delta x_0)$$

The term can be considered as the length of an input object (Here, we only consider the one dimensional case.)

The Fresnel transform for the far field regime – 1

- For the far-field regime, the Fresnel transform is given as

$$u_z\left(r\Delta x_z\right)=\exp\left\{\frac{j\pi}{\lambda z}\left(r\Delta x_z\right)^2\right\}\times\mathcal{F}\left[u_{in}\left(q\Delta x_0\right)\exp\left\{\frac{j\pi}{\lambda z}\left(q\Delta x_0\right)^2\right\}\right]$$

- To comply with standard CS formulations, the Fresnel transform is represented in a vector-matrix form:

$$\mathbf{u}_z=\mathbf{Q}_{\Delta x_z}\mathbf{F}\mathbf{Q}_{\Delta x_0}\mathbf{u}_{in}=\mathbf{\Phi}^{FF}\mathbf{u}_{in}$$

$$\mathbf{Q}_{\Delta x_z}=diag\left[\exp\left(\frac{j\pi}{\lambda z}\left(\Delta x_z\right)^2\right)\quad\exp\left(\frac{j\pi}{\lambda z}\left(2\Delta x_z\right)^2\right)\quad\cdots\quad\exp\left(\frac{j\pi}{\lambda z}\left(n\Delta x_z\right)^2\right)\right]$$

$$\mathbf{Q}_{\Delta x_o}=diag\left[\exp\left(\frac{j\pi}{\lambda z}\left(\Delta x_o\right)^2\right)\quad\exp\left(\frac{j\pi}{\lambda z}\left(2\Delta x_o\right)^2\right)\quad\cdots\quad\exp\left(\frac{j\pi}{\lambda z}\left(n\Delta x_o\right)^2\right)\right]$$

$\mathbf{F}$ is the Fourier transform matrix

The Fresnel transform for the far field regime – 2

- Since the matrix Φ^{FF} is the Fourier transform matrix and remaining matrices are phase matrices, the mutual coherence for the far-field case is one.
- Thus, the number of measurements are represented by

$$m\geq Cs\log n$$

- This results means that the distance *has no effect* on the sparse signal reconstruction guaranties, and *it behaves exactly as compressive Fourier* sensing.

The Fresnel transform for the near field regime

- For the near field regime, the Fresnel transform is represented in a vector-matrix form:

$$\mathbf{u}_z = \mathbf{F}^{-1}\tilde{\mathbf{Q}}_{\Delta x_0}\mathbf{F}\mathbf{u}_{in} = \mathbf{\Phi}^{NF}\mathbf{u}_{in}$$

$$\tilde{\mathbf{Q}}_{\Delta x_0} = diag\left[\exp\left(\frac{j\pi\lambda z}{(n\Delta x_0)^2}\right) \quad \exp\left(\frac{j\pi\lambda z 2^2}{(n\Delta x_0)^2}\right) \quad \cdots \quad \exp\left(\frac{j\pi n^2}{\lambda z}\right)\right]$$

- For the one-dimensional case, the mutual coherence is

$$\mu_{1D} \approx n\frac{\Delta x_0^2}{\lambda z}.$$

- The mutual coherence for the two-dimensional case is

$$\mu_{2D} \approx n^2\left(\frac{\Delta x_0^2}{\lambda z}\right)^2 = N\left(\frac{\Delta x_0^2}{\lambda z}\right)^2$$

- Then, the number of measurements are represented by

$$m \geq Cn\left(\frac{\Delta x_0^2}{\lambda z}\right)s\log n \text{ or } m \geq CN\left(\frac{\Delta x_0^2}{\lambda z}\right)^2 s\log N$$

Conclusions

- For the far field case, the distance *has no effect* on the number of measurements.

$$m \geq Cs\log N$$

- For the near field case, the distance *has effect* on the number of measurements. Also, the object resolution element size *has effect* on the number of measurements.

$$m \geq Cn\left(\frac{\Delta x_0^2}{\lambda z}\right)s\log n \text{ or } m \geq CN\left(\frac{\Delta x_0^2}{\lambda z}\right)^2 s\log N$$

- But, we remind that the object resolution element size must satisfy the below relation

$$\Delta x_z = \lambda z/(n\Delta x_0)$$

Random-Frequency SAR Imaging Based on Compressed Sensing

J. Yang et al.

IEEE Trans. Geo. Remot. Sensing (2013. Feb.)

Presenter : Jin-Taek Seong

GIST, Dept. of Information and Communications, INFONET Lab.

Gwangju Institute of Science and Technology

Introduction

- The stepped-frequency waveform consists of sequences of single-frequency pulses
- The stepped-frequency waveform can be viewed as the frequency sampling of the total bandwidth
- The advantages of a single frequency
  - Simple hardware requirements
  - High resolution
- The drawback is
  - A long time period to transmit the signals, since the transmitter must scan over the radar bandwidth using a sequence of discrete frequencies
- Therefore, this leads to many limitations for the application of the stepped-frequency waveform in SAR.
- There has to be a tradeoff between the resolution and imaging range width.

Introduction

- If the targets are sparse or compressible, the required frequencies in the stepped-frequency SAR can be reduced significantly using a CS theory
- In this paper, a random-frequency SAR imaging scheme based on CS is proposed
  - Reconstruction the 2-D image of the sparse targets by transmitting a small number of random frequencies.
- A sparse transform structure is proposed for the reshaped 2-D reflectivity map.
- The main advantages of the proposed imaging scheme
  - 1) the available imaging range width can be enlarged significantly, while the range and azimuth resolutions are both maintained
  - 2) the required number of frequencies can be reduced
  - 3) random undersampling is very easy to implement for both range and azimuth

Stepped-Frequency Waveform (1/2)

- The stepped-frequency waveform uses a sequence of pulses to achieve an ultrawide bandwidth
- We denote the transmitted waveform as

$$s_t(n,t) = \text{rect}\left(\frac{t}{T_p}\right)\exp\left[j2\pi f_c(n)t\right] \qquad (1)$$

- For a point reflector at range *R*, the echo signal is

$$s_e(n,t) = g\cdot\text{rect}\left(\frac{t-2R/c}{T_p}\right)\exp\left[j2\pi f_c(n)(t-2R/c)\right] \qquad (2)$$

  - *g* is the reflectivity coefficient of the target
- The demodulation reference signal is

$$\begin{aligned} s(n,t) &= s_e(n,t)\cdot s_{\text{ref}}^*(n,t) \\ &= g\cdot\left(\frac{t-2R/c}{T_p}\right)\exp\left[j2\pi f_c(n)(t-2R/c)\right] \\ &\quad\cdot\exp\left[-j2\pi f_c(n)t\right] \\ &= g\cdot\text{rect}\left(\frac{t-2R/c}{T_p}\right)\exp\left[-j\frac{4\pi f_c(n)R}{c}\right] \end{aligned} \qquad (4)$$

Stepped-Frequency Waveform (2/2)

- We consider that the frequency interval is equal to Δ*f*, so that

$$f_c(n) = f_c + n\Delta f, \qquad n = 1, 2, \ldots N \qquad (5)$$

- The demodulated signal can be rewritten as

$$s(n,t) = g \cdot \text{rect}\left(\frac{t - 2R/c}{T_p}\right) \exp\left[-j\frac{4\pi(f_c + \Delta f n)R}{c}\right]. \qquad (6)$$

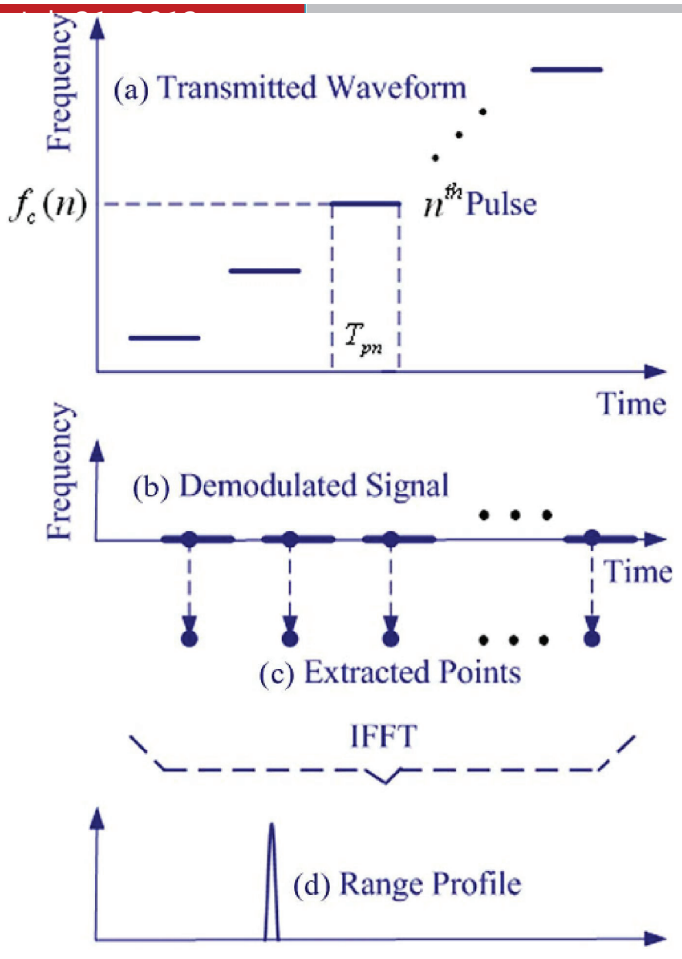

Fig. 1. Processing of stepped-frequency waveform. (a) Transmitted waveform. (b) Demodulated signal. (c) Extracted data points. (d) Range profile.

Limitations of Stepped-Frequency Waveform Applied to SAR (1/2)

- Sampling with Δ*f* results in periodic repetition in the time domain, and the repetition period is 1/Δf
- The corresponding repetition period for range is *c*/(*2Δf*), so the nonaliasing range width is limited to

$$R_w < \frac{c}{(2\Delta f)} \tag{8}$$

- For a fixed pulse time interval, to avoid overlapping of the echoes, the maximum range width is

$$D_1 = \frac{\Delta tc}{2} \tag{9}$$

- For a given frequency step, the maximum nonaliasing range width is

$$D_2 = \frac{c}{2\Delta f} = \frac{Nc}{2B} \tag{10}$$

- Therefore, the **maximum available range width** is

$$D = \min\{D_1, D_2\}. \tag{12}$$

Limitations of Stepped-Frequency Waveform Applied to SAR (2/2)

- The equivalent azimuth sampling interval is *NΔtV*, where *V* is the radar velocity.

$$r_a = N\Delta tV. \tag{13}$$

- The range resolution is

$$r_r = \frac{c}{2B}. \tag{14}$$

- The available imaging range width and the range resolution and azimuth resolution must be traded off against each other
- To let the available range width become wider, *Δt* and *N* should be bigger, *B* should be smaller, but all of these requirements will decrease the resolution in both the range and azimuth dimensions.

Random-Frequency SAR Imaging Based on CS-SAR Imaging Model (1/3)

- The radar data are the superposition of the echoes of all scatterers in the area illuminated by the radar's beam (i.e., the scene)
- The received signal of the *n*th pulse in the *m*th sequence can be expressed as

$$s(m,n) = \iint_G g(x,y) \cdot \exp\left[-j\frac{4\pi f_c(n) R(m,n,x,y)}{c}\right] dxdy$$

  - x and y are the coordinates of the target
  - *g*(x, y) is the reflectivity coefficient of the target at (x, y)
  - *R*(m, n, x, y) is the range of the target at (x, y)
  - *G* is the area illuminated by the beam

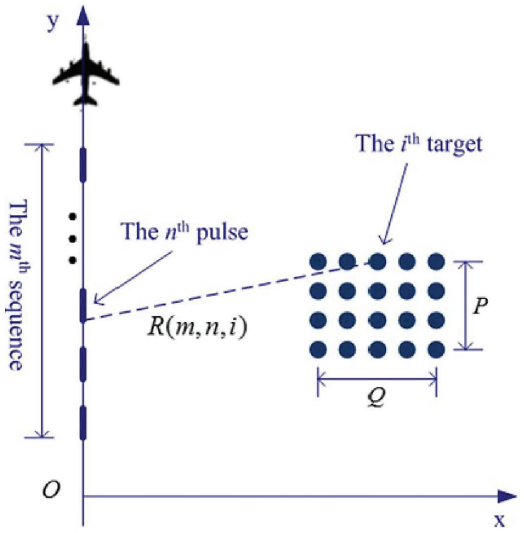

Fig. 2. Geometry model for SAR imaging.

Random-Frequency SAR Imaging Based on CS-SAR Imaging Model (2/3)

- The scene consists of a set of point scatterers on a grid, and the interval of the grids should be smaller than the radar resolution
- The reflectivity coefficients of the scatterers can be denoted as a 2-D matrix

$$\mathbf{G} = \begin{bmatrix} g(1,1) & \cdots & g(1,Q) \\ \vdots & \ddots & \vdots \\ g(P,1) & \cdots & g(P,Q) \end{bmatrix}$$

- The 2-D reflectivity coefficient matrix should be reshaped to a column vector, i.e., *g* is a PQ × 1 vector
- The discrete expression of the radar data of the *n*th pulse in the *m*th sequence is

$$s(m,n) = \sum_{i=1}^{PQ} g(i) \cdot \exp\left[-j\frac{4\pi f_c(n) R(m,n,i)}{c}\right]$$

Random-Frequency SAR Imaging Based on CS-SAR Imaging Model (3/3)

- The linear equation can be expressed in matrix form as

$$\mathbf{s} = \mathbf{A}\mathbf{g} + \mathbf{n}$$

  - where *s* is an *MN*×1 vector, *A* is an *MN*×*PQ* matrix, *g* is a *PQ*×1 vector, and *n* is the noise term. *M* is the total number of sequences; *N* is the number of frequencies in one sequence.

- The detailed form is

$$\mathbf{s}=\begin{bmatrix} s(1,1) \\ \vdots \\ s(1,N) \\ s(2,1) \\ \vdots \\ s(2,N) \\ \vdots \\ s(M,1) \\ \vdots \\ s(M,N) \end{bmatrix} = \mathbf{A}\mathbf{g}+\mathbf{n} = \begin{bmatrix} \mathbf{a}(1,1)^{\mathrm{T}} \\ \vdots \\ \mathbf{a}(1,N)^{\mathrm{T}} \\ \mathbf{a}(2,1)^{\mathrm{T}} \\ \vdots \\ \mathbf{a}(2,N)^{\mathrm{T}} \\ \vdots \\ \mathbf{a}(M,1)^{\mathrm{T}} \\ \vdots \\ \mathbf{a}(M,N)^{\mathrm{T}} \end{bmatrix} \begin{bmatrix} g(1) \\ g(2) \\ \vdots \\ g(PQ) \end{bmatrix} + \mathbf{n}.$$

Random-Frequency SAR Imaging Based on CS-CS Imaging Scheme

- In order to apply a CS scheme, a reduced set of elements in *s* is selected randomly, and a reduced set of rows in *A* is also selected accordingly. It means that a small number of frequencies are selected randomly.

- The CS measurement can be expressed as

$$\mathbf{s}' = \mathbf{A}'\mathbf{g} + \mathbf{n}'$$

- The targets can be reconstructed as

$$\min \|\mathbf{g}\|_1 \quad s.t. \quad \|\mathbf{A}'\mathbf{g} - \mathbf{s}'\|_2 \leq \varepsilon.$$

- Assume that *L* samples are selected from the total of *MN* samples; then, the uniform pulse time interval becomes (*MN*/*L*)*Δt*, so that the maximum available range width becomes

$$D' = \frac{MN}{L}\frac{\Delta tc}{2}.$$

Random-Frequency SAR Imaging Based on CS-Sparsity of Targets

- A Priori Sparse Targets: it means that the targets consist of a small number of dominant scatterers
- Sparsely Representable Targets: we can find a transform to make most of the coefficients in the transform domain
- The CS imaging scheme combined with the sparse transform (see the appendix) can be expressed as

$$\mathbf{s}' = \mathbf{A}'\mathbf{g} + \mathbf{n}' = \mathbf{A}'(\tilde{\mathbf{\Psi}}_r\tilde{\mathbf{\Psi}}_c)^{-1}\tilde{\mathbf{\Psi}}_r\tilde{\mathbf{\Psi}}_c\mathbf{g} + \mathbf{n}'.$$

- This equation can be rewritten as

$$\mathbf{s}' = \mathbf{A}'(\tilde{\mathbf{\Psi}}_r\tilde{\mathbf{\Psi}}_c)^{-1}\mathbf{x} + \mathbf{n}'.$$

- We can solve for the transform coefficients using

$$\hat{\mathbf{x}} = \min \|\mathbf{x}\|_1 \quad s.t. \quad \left\|\mathbf{A}'(\tilde{\mathbf{\Psi}}_r\tilde{\mathbf{\Psi}}_c)^{-1}\mathbf{x} - \mathbf{s}'\right\|_2 \le \varepsilon.$$

- Then, the reflectivity coefficients can be obtained by

$$\hat{\mathbf{g}} = (\tilde{\mathbf{\Psi}}_r\tilde{\mathbf{\Psi}}_c)^{-1}\hat{\mathbf{x}}.$$

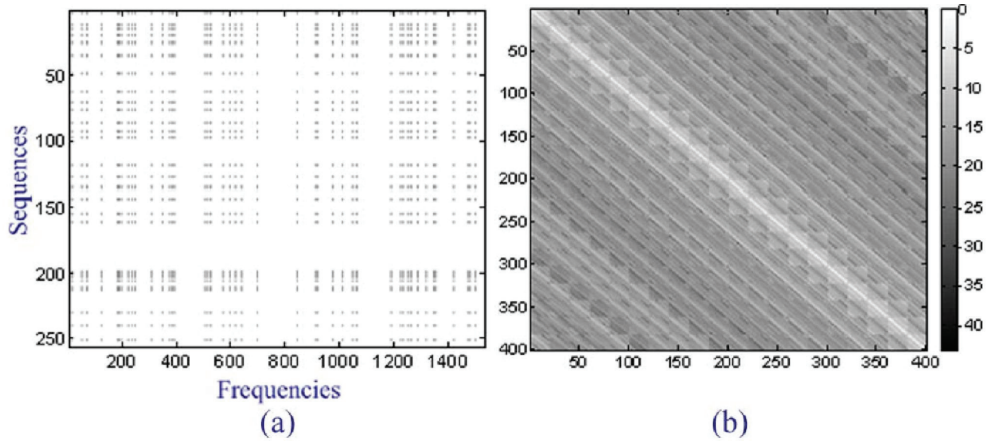

Fig. 3. Selected samples and mutual coherences for Option 1. (a) Selected samples. (b) Mutual coherences of the sensing matrix (scaled in decibels).

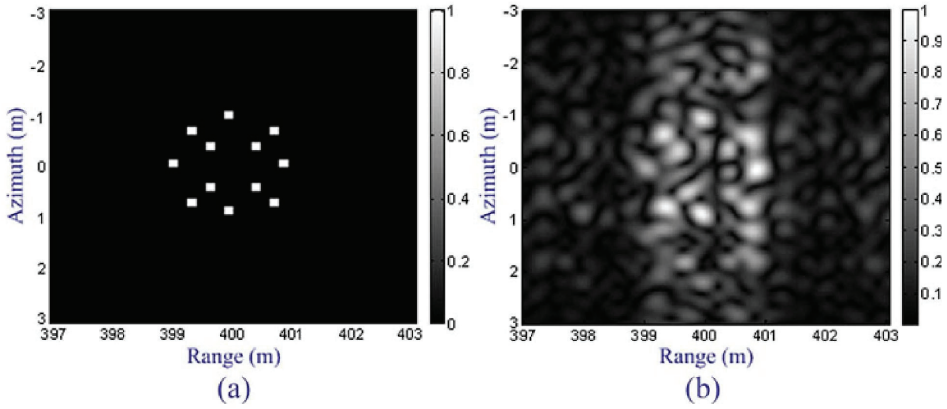

Fig. 6. Results of Option 1. (a) CS reconstruction result of the 1/192 data. (b) Imaging result of the 1/192 data using the Omega-K algorithm.

Experimental Results

- In order to show the validity, an experiment is carried out for stepped-frequency and random-frequency SAR imaging
- A stepped-frequency radar is mounted on a rail to acquire data
- The rail is controlled by a microcomputer, and the radar can move on the rail with a preset velocity

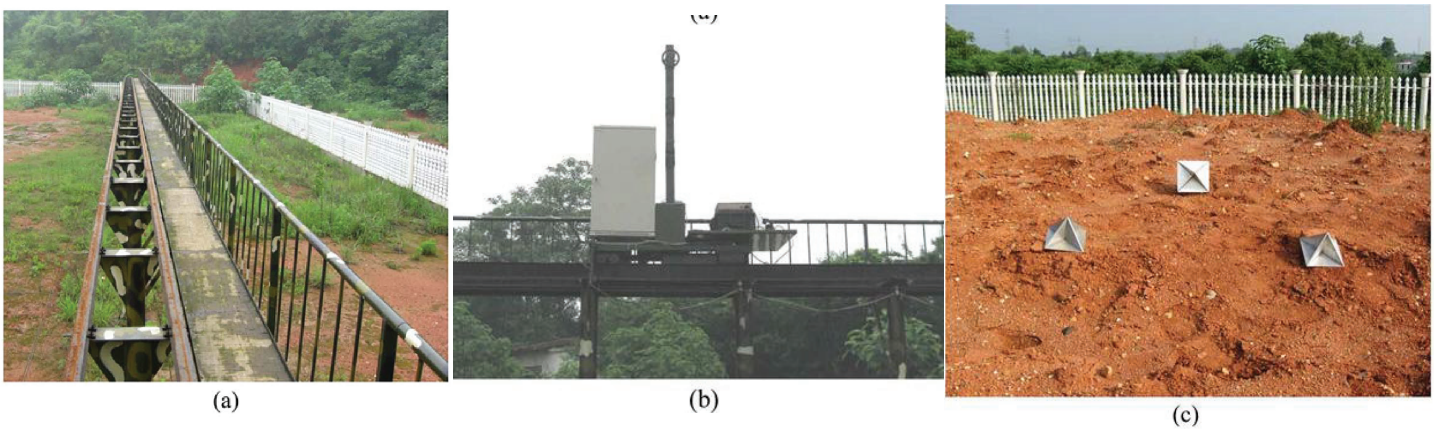

(a) (b) (c)

TABLE II
EXPERIMENT PARAMETERS

Bandwidth	512MHz
Pulse Time Interval	1e-3s
Radar Velocity	0.05m/s
Squint Angle	0°
Range Resolution	0.293m
Azimuth Resolution	0.05m
Number of Frequencies	512
Number of Sequences	480
Scene Azimuth Points	40
Scene Range Points	20
Selected Samples for CS	1024

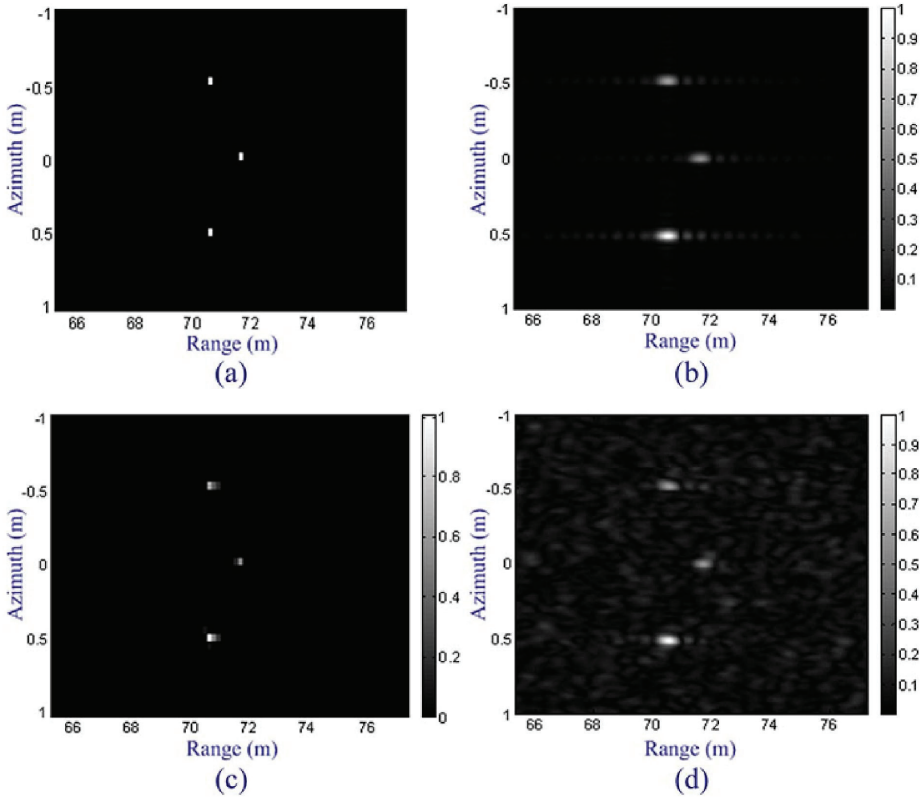

Fig. 12. Experimental results. (a) Position of the three corner reflectors. (b) Imaging result of the full data using the Omega-K algorithm. (c) CS reconstruction result of 1/240 data. (d) Imaging result of 1/240 data using the Omega-K algorithm.

Conclusions

- The theory of CS has been used to reduce the required frequencies in a stepped-frequency SAR system
- Based on the theory of CS, the traditional sampling requirements can be avoided, and the limitations of the stepped-frequency waveform applied in SAR are overcome
- The available imaging range width can be enlarged significantly, while the range and azimuth resolutions are maintained.
- The results of the CS imaging scheme are even better than the traditional results of the fully sampled data
- Future work will include fast reconstruction strategies and detailed investigations of the sparsity and compressibility of the targets
- Speckle noise will make the phase of the reflectivity map random, and it is difficult to find an effective sparse transform for a complex reflectivity map

Appendix – Transform of the 2D Matrix

- We begin with the sparse transform for the 2-D reflectivity matrix. The sparse transform can be applied to both the columns and rows of the 2-D matrix, and it can be expressed as.

$$\mathbf{X} = \mathbf{\Psi}_c \mathbf{G} \mathbf{\Psi}_r$$

  - where X contains the coefficients after the sparse transform, G is shown in (29), Ψ_c is the sparse transform matrix for the columns, the size of Ψ_c is $P \times P$, Ψ_r is the sparse transform matrix for the rows, and the size of Ψ_r is $Q \times Q$. Ψ_c and Ψr are full rank matrices.
- In the imaging scheme based on CS, the 2-D reflectivity matrix G is reshaped to a column vector g

$$\tilde{\mathbf{\Psi}}_c = \begin{bmatrix} \mathbf{\Psi}_c & & & \\ & \mathbf{\Psi}_c & & \\ & & \ddots & \\ & & & \mathbf{\Psi}_c \end{bmatrix} \qquad \tilde{\mathbf{\Psi}}_r = \begin{bmatrix} \mathbf{\Psi}_{r1} \\ \mathbf{\Psi}_{r2} \\ \vdots \\ \mathbf{\Psi}_{ri} \end{bmatrix}$$

- The sparse transform of the reshaped reflectivity vector can be expressed as

$$\mathbf{x} = \tilde{\mathbf{\Psi}}_r \tilde{\mathbf{\Psi}}_c \mathbf{g}$$